

Intraseasonal modulation of tropical cyclogenesis in the western North Pacific: a case study

Jiangyu Mao · Guoxiong Wu

Received: 16 February 2009 / Accepted: 29 June 2009 / Published online: 23 August 2009
© Springer-Verlag 2009

Abstract The temporal clustering of the western North Pacific tropical cyclogenesis and its modulation by the Madden–Julian oscillation (MJO) during the 1991 summer were examined based on the tropical cyclone best track, outgoing longwave radiation, and NCEP/NCAR reanalysis datasets. The wavelet analysis shows that convective activities around the monsoon trough in the western North Pacific possessed a distinct MJO with a period of 20–60 days. Two or more tropical cyclones were observed to form successively during each active phase of the MJO, and tropical cyclones tended to generate around the southeastern part of the maximum vorticity of the low-frequency cyclonic circulation during the developing and peak stages of the active MJO phase. But tropical cyclogenesis scarcely occurred during inactive MJO phases. Thus the MJO was a major agent in modulating repeated development of tropical cyclones in the western North Pacific during the 1991 summer. The MJO in circulation was characterized by a huge anomalous cyclone (anticyclone) in the lower troposphere existing alternately over the western North Pacific, leading to an enhanced (weakened) monsoon trough. An examination of the meridional gradient of absolute vorticity associated with the zonal flow indicates that the zonal flow in the monsoon trough region satisfied the necessary conditions for barotropic instability, with both zonal flow and the meridional gradient of absolute vorticity varying on the similar MJO timescale. The intraseasonal oscillation of such an unstable zonal flow might thus be an important

mechanism for temporal clustering of tropical cyclogenesis in the western North Pacific. The barotropic conversion could provide a major energy source for the formation and growth of tropical cyclones in the western North Pacific during active MJO phases, with the eddy kinetic energy generation being dominated by both terms of eddies interacting with zonal and meridional gradients of the basic zonal flow.

1 Introduction

The western North Pacific contains much warm ocean water over a broad area; thus, it is the most active basin of tropical cyclogenesis (Gray 1968; McBride 1995). Tropical cyclones may form during any month of the year, but they mostly occur in summer and fall. A number of mechanisms have been proposed for tropical cyclogenesis in the western North Pacific. Some studies (e.g., Gray 1968; Ding et al. 1977; Zehr 1992) have shown that the majority of the tropical cyclones in the western North Pacific develop within the monsoon trough that is typically a convergence zone between monsoon westerlies and trade easterlies in a band extending southeastward from the South China Sea into the east of the Philippine Sea. Tropical cyclone formations are further found to be associated with synoptic-scale disturbances such as mixed Rossby gravity (MRG) wave and “tropical depression-type (TD)” mode in the monsoon trough (Takayabu and Nitta 1993; Chen and Weng 1998; Molinari et al. 2000). Most of these disturbances are present around the eastern end of the trough (Briegel and Frank 1997; Holland 1995). McBride and Zehr (1981) found enhanced relative vorticity in the lower troposphere on a 1,000–2,000-km scale in the environment of cloud clusters that develop into tropical cyclones,

J. Mao (✉) · G. Wu
State Key Laboratory of Numerical Modeling for Atmospheric Sciences and Geophysical Fluid Dynamics (LASG),
Institute of Atmospheric Physics, Chinese Academy of Sciences,
P.O. Box 9804, Beijing 100029, China
e-mail: mjoy@lasg.iap.ac.cn

compared to non-developing clusters. Chang et al. (1996) identified periods of enhanced northwestward-moving disturbances with the presence of one or more tropical cyclones in the monsoon trough. The consecutive tropical cyclone formations may be related to the MRG wave packet. Dickinson and Molinari (2002) showed that tropical cyclogenesis tends to occur in the cyclonic part of disturbances that are making the transition from MRG to TD type. It has been argued that the easterly waves could grow in the western North Pacific where trade easterlies meet monsoon westerlies via Rossby wave accumulation, essentially convergence of the group velocity (Holland 1995; Sobel and Bretherton 1999).

In addition to the synoptic-scale disturbances, the large-scale Madden–Julian oscillation (MJO; Madden and Julian 1994) has been recognized to influence the western Pacific tropical cyclogenesis (e.g., Gray 1979; Liebmann et al. 1994). The MJO is a global-scale eastward propagating wave-like disturbance of the tropical atmosphere whose period varies between 30 and 80 days (Wheeler and Hendon 2004), with most frequent occurrence around 45 days (Madden and Julian 1994). The MJO signal is observed in both the flow and convection fields with coherent fluctuations in winds and convective activities (e.g., Zhang 2005) and with large convection variance mostly confined to the eastern Indian Ocean and western Pacific sectors (Wheeler and Kiladis 1999; Fu et al. 2000). Gray (1979) found that globally there are 1–2 weeks of active cyclogenesis, followed by 2–3 weeks of quiescence. In investigating the intraseasonal behaviors of tropical outgoing longwave radiation (OLR) during 1979 (the FGGE year), Nakazawa (1986) noted that the generation and growth of tropical cyclones tend to occur during the active phase of 30–60-day filtered convection anomalies. Based on the 11-year data of 1979–1989, Liebmann et al. (1994) showed that tropical cyclones over the Indian and western Pacific Oceans preferentially occur during the convective phase of the MJO and cluster around the low-level cyclonic vorticity and convergence anomalies that appear pole- and westward of the large-scale convective anomaly along the equator. Similar modulation of tropical cyclone activity by the MJO was found in the Australian region (Hall et al. 2001) and in the south Indian Ocean region (Bessafi and Wheeler 2006). The synoptic-scale (periods 2–15 days) convective activity increases by 50–100% in the wet phase of the MJO compared to the dry phase (Hendon and Liebmann 1994). A pronounced cycle in the number of named tropical systems (hurricanes and tropical storms) was found to occur in the eastern Pacific during a composite life cycle of the MJO (Maloney and Hartmann 2000), with hurricanes and tropical storms during the period of equatorial 850-hPa westerly anomalies being over twice as many as those during the period of easterly

anomalies. In examining the linkage between the temporal clustering of tropical cyclogenesis and the MJO, Harr (2006) found that in years with significant MJO events, there is a statistically significant increase in the probability of tropical cyclone activity during the active convective phases and a statistically significant reduction during the inactive convective phases. Dickinson and Molinari (2002) showed a clear sequence of events that incorporated the MJO, the MRG wave, and tropical cyclogenesis, with the MRG wave packet first appearing coincidentally with the arrival of the MJO. The packet amplified as long as it remained within the active MJO and quickly dispersed when the MJO moved eastward and left it behind.

Tropical cyclogenesis in most ocean basins has a strong interannual variability (Landsea 2000), and such an interannual variability in the western North Pacific is associated with the state of the El Niño–Southern Oscillation (ENSO; e.g., Chan 2000). It is well known that the period 1991–1993 was characterized by a prolonged El Niño episode. This El Niño event really began around early May of 1991, with warm sea surface temperature (SST) anomalies exceeding 0.5°C in the central and eastern Pacific and reached its peak phase in the first quarter of 1992 (McPhaden 1993). The 1991 summer thus coincided with the developing phase of the El Niño event. At the same time, devastating flood took place over the Yangtze Basin in China during this summer. More noteworthy, three typhoons (namely Zeke, Amy, and Brendan) formed consecutively in the western North Pacific, and they all made landfall in southern China during July, exhibiting an unusual activity of tropical cyclones and leading to more severe economic loss. Another significant feature was that during this summer, tropical cyclogenesis in the western North Pacific exhibited striking fluctuations in the frequency with several distinct active and inactive periods. Actually, Molinari et al. (1997) noted that during the 1991 summer, tropical cyclogenesis in the eastern North Pacific also possessed remarkable intraseasonal variability and conducted a case study to examine the role of easterly waves played in the eastern North Pacific tropical cyclogenesis due to unstable basic flow. They suggested that upstream wave growth in the dynamically unstable region provides a connection between the MJO and the associated enhanced downstream tropical cyclogenesis.

Hendon et al. (1999) found that the characteristics of the MJO can be altered by the phase of ENSO, and Hall et al. (2001) noted the modulation of tropical cyclone activity by the MJO being strengthened during El Niño periods in the northern Australia. These suggest that similar strong modulation associated with El Niño event may exist in the western North Pacific because ENSO was found to affect the intensity and location of the monsoon trough (Chen et al. 1998). In view of significant intraseasonal

variations of tropical cyclogenesis and unusual features in terms of consecutive landfall of typhoons and the El Niño background, the 1991 summer was thus selected to investigate intraseasonal behaviors of tropical cyclogenesis in the western North Pacific through a detailed analysis on the tropical atmospheric circulation associated with the MJO, which may provide some information for understanding the causes of extreme weather and climate events related to interannual variations.

Based on the necessary conditions for tropical cyclogenesis (Gray 1968, 1979), Liebmann et al. (1994) suggested that the clustering of tropical cyclogenesis may result from the episodic occurrence of favorable large-scale environmental conditions. Associated with these favorable conditions, the role of barotropic dynamics to eddy kinetic energy growth has been noted in tropical cyclogenesis regions during active MJO phases (Hartmann and Maloney 2001). Maloney and Hartmann (2000) suggested that when the MJO wave propagates eastward from the western Pacific, westerly (easterly) wind anomalies over the eastern Pacific occur near the hurricane genesis region, with anomalous cyclonic (anticyclonic) horizontal shear of the low-level zonal wind and low (high) vertical wind shear. The MJO thus modulates hurricane activity by creating favorable conditions for development or suppression of tropical cyclones in the eastern Pacific. When 850-hPa wind anomalies of the MJO are westerly in the eastern or western North Pacific, synoptic-scale disturbances grow through barotropic eddy kinetic energy conversion from the mean flow (Maloney and Hartmann 2001). In support of these results, the observational study (Norquist et al. 1977) suggested that barotropic energy conversions from mean flow are crucial to the formation of the most unstable easterly waves near the African easterly jet. The idealized modeling simulations by Thorncroft and Hoskins (1994a, 1994b) showed that both barotropic and baroclinic processes contribute to easterly wave growth. The above results imply that a similar modulation of tropical cyclogenesis by the MJO may exist in the western North Pacific because the fluctuation of westerlies and easterlies in the monsoon trough influences the horizontal shear of the low-level zonal wind.

As suggested by Maloney and Hartmann (2001), barotropic dynamics may help to explain the modulation of western North Pacific tropical cyclone formations by the MJO during boreal summer since the strong low-level convergence, cyclonic shear, and growing disturbance in the monsoon trough along with high SST create a favorable environment for tropical cyclogenesis. Therefore, the purpose of this research is to identify the intraseasonal modulation of tropical cyclogenesis in the western North Pacific and to examine the importance of barotropic dynamics for eddy kinetic energy growth during active MJO phases.

Data and methods used for this study are briefly described in Section 2. The characteristics of intraseasonal variations in tropical convection and cyclogenesis are investigated in Section 3. The successive occurrences of tropical cyclones within an active MJO phase in association with low-frequency circulation are presented in Section 4. Intraseasonal fluctuations of the barotropically unstable zonal flow in the region of the monsoon trough are identified in Section 5. Contributions of the unstable basic flow to the growth of synoptic disturbances through barotropic eddy-mean flow interactions are examined in Section 6. Summary and discussion are given in Section 7.

2 Data and methods

2.1 Data

The primary circulation data used in this study for the year 1991 are daily products extracted from the National Centers for Environmental Prediction/National Center for Atmospheric Research (NCEP/NCAR) reanalysis (Kalnay et al. 1996), with a horizontal resolution of 2.5° latitude–longitude grid. Daily OLR data (Liebmann and Smith 1996), which are extracted from the National Oceanic and Atmospheric Administration (NOAA) with the same resolution as the NCEP/NCAR reanalysis data, are used as a proxy for large-scale tropical convective activity. The long-term daily mean climatology is based on the daily OLR data for the period 1979–1995, and it is obtained directly from the website of NOAA-CIRES Climate Diagnostics Center to confirm the amount of subseasonal variability during the 1991 summer. Since the MJO is characterized by the large-scale eastward propagation of OLR anomalies (Madden and Julian 1994), the MJO and convectively coupled wave signatures in the tropics can be identified based on OLR fields (Wheeler and Kiladis 1999). In this study, OLR data are used to investigate the intraseasonal behaviors associated with the MJO in the western North Pacific.

Tropical cyclone data for the period 1961–2004 on the best track and origin are obtained from Shanghai Typhoon Institute of China Meteorological Administration, including the position in latitude and longitude, maximum sustained wind speed, and central pressure of the tropical cyclone at 6-h interval. In the present study, tropical cyclones include all named and unnamed systems from tropical depressions to typhoons, unless otherwise stated. Such data have been used to examine the influences of tropical cyclones on annual rainfall over southeastern China and their interannual changes (e.g., Ren et al. 2006).

2.2 Wavelet analysis and filtering

Wavelet analysis is a common tool for diagnosing time–frequency variations of a time series, with a practical guide to this method given by Torrence and Compo (1998). Thus the wavelet analysis is used in this study to identify the dominant intraseasonal oscillations, as was done in Mao and Chan (2005). The time series of the intraseasonal components are reconstructed by the inverse transform over a range of scales since the wavelet transform is also a powerful filtering technique (Torrence and Compo 1998; Chan et al. 2002). Because the temporal variation of tropical convection generally exhibits significant oscillatory behavior with sharp jump, based on the choice principle of the wavelet function, the wavelet basis function selected here is the sixth-order derivatives of a Gaussian function (Torrence and Compo 1998). Such a real wavelet function returns only a single component and is suitable to isolate peaks or discontinuities. The gridded fields of other daily meteorological quantities such as 850-hPa winds are also filtered with the same wavelet transform to extract the intraseasonal components. To get more accurate results for both frequency and filtered component, the time series such as daily OLR used for wavelet analysis is extended, respectively, forward and backward by a month in order to reduce the edge effects (Torrence and Compo 1998) at the beginning and end of the time series. In present study, the daily anomaly data from May to October in 1991 were applied to wavelet transform to identify the intraseasonal variations for the period June–September.

3 Intraseasonal variations in tropical convection and cyclogenesis

Previous studies have shown that most of tropical cyclones occur during months of June to September in the western North Pacific; the period June–September is thus the major typhoon season (Chen and Ding 1979; Kim et al. 2008). Based on the tropical cyclone statistics for the period 1961–2004, climatologically, the annual number of tropical cyclones is 34 in the western North Pacific along with the South China Sea, and 22 of these cyclones occur from June to September, accounting for 64.7% of total cyclogenesis.

In 1991, there were 29 named and two unnamed tropical cyclones generated in the western North Pacific and South China Sea, with 18 of these cyclones forming during summer season (here refers to June–September), indicating that the summertime was also major season of tropical cyclogenesis in 1991. Although the number of tropical cyclones during the 1991 summer was somewhat less than that in climatology, most of these cyclones spatially generated around the monsoon trough, especially their

occurrences temporally displayed distinct active and inactive periods. Therefore, in this research, we focus on the temporal clustering of tropical cyclogenesis.

To show how anomalous the convective activity was during the 1991 summer, Fig. 1 displays the distribution of subseasonal standard deviations of OLR. The standard deviation for each grid point is calculated based on the daily OLR anomaly, and this anomaly is defined as the departure from the long-term daily mean climatology for the period 1 June to 30 September. Larger deviations above 40 W m^{-2} were found to cover a much large area from the South China Sea to the western North Pacific, with the entire area being almost separated into two regions by the Philippines, indicating strong intraseasonal and synoptic-scale variability associated with tropical cyclone activity. We have also calculated the standard deviations with daily OLR anomalies relative to the average for the period 1 June to 30 September 1991. Similar distribution is obtained except for standard deviation maxima slightly larger than those shown in Fig. 1, indicating that under the circumstance of small climatological seasonal trend the subseasonal variability for a particular summer can be estimated based on the departure from the average of this summer itself for a case study.

Harr and Elsberry (1995) pointed out that beyond the SST distribution in the western North Pacific, the location of the monsoon trough exhibits primary control over the distribution of tropical cyclone activity in this basin. The vicinity of the monsoon trough is the main genesis region for tropical cyclones due to strong convergences between westerlies and easterlies and positive vorticity-rich low-level environments (Gray 1968; McBride 1995). Note that

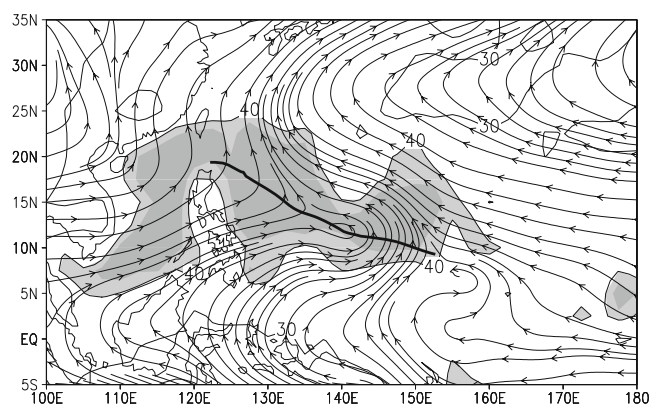


Fig. 1 The distributions of seasonal mean (June–September) 850-hPa winds (streamline, m s^{-1}) and subseasonal standard deviations of OLR (contour, W m^{-2}) for the 1991 summer. Daily OLR anomalies during the 1991 summer are calculated as departures from the 1979–1995 base period climatological daily means from 1 June to 30 September. The standard deviations greater than 40 and 43 W m^{-2} are *lightly* and *heavily shaded*, respectively. The monsoon trough is *highlighted by thick solid curve*

the distribution of maximum deviations in excess of 43 W m^{-2} in the western North Pacific exhibited a northwest–southeast orientation, with the core area of maximum deviations coinciding with the monsoon trough (Fig. 1).

To highlight the intraseasonal variation in tropical cyclogenesis during the summer of 1991, Fig. 2 presents time-latitude cross sections of daily OLR and 850-hPa relative vorticity averaged along $125\text{--}155^\circ\text{E}$, with initial positions of tropical cyclogenesis superimposed. From the beginning of June and thereon, there were four deep convection episodes with OLR values less than 220 W m^{-2} , indicating that well-organized convective clouds produced quasi-periodically and extended northward. Note that tropical cyclones mostly generated during deep convection phases (Fig. 2a), with remarkable intraseasonal oscillations in the frequency of cyclogenesis. Correspondingly, strong positive relative vorticity in the lower troposphere also exhibited distinct fluctuations on the similar intraseasonal timescale (Fig. 2b). Actually, such a large-scale low-level cyclonic vorticity in the environment of deep convection was one of the necessary conditions for tropical cyclogenesis (Gray 1968).

As shown in Figs. 1 and 2, area-averaged OLR over the western North Pacific ($7.5\text{--}20^\circ\text{N}$, $125\text{--}155^\circ\text{E}$) is defined as an index to identify the intraseasonal variability. This area used for average is chosen because it contains maximum standard deviations. The anomaly of this OLR index is shown in Fig. 3, and the wavelet analysis is applied to this anomaly time series to identify the dominant intraseasonal

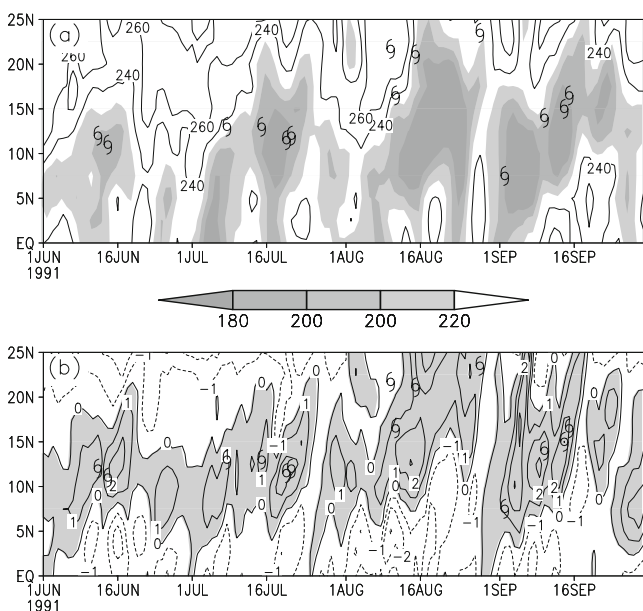


Fig. 2 Time-latitude cross sections of zonally averaged ($125\text{--}155^\circ\text{E}$) daily **a** OLR (W m^{-2}) and **b** 850-hPa relative vorticity (s^{-1}). In **a**, *shadings* denote OLR values less than 220 W m^{-2} , and *contours* indicate OLR values greater than 220 W m^{-2} . In **b**, positive vorticity areas are *shaded*. The typhoon symbols indicate the times and latitudes of initial formation of tropical cyclones

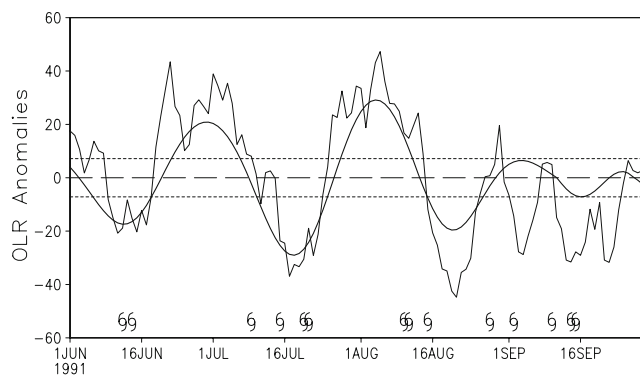


Fig. 3 Time series of area-averaged OLR anomalies over the western North Pacific ($7.5\text{--}20^\circ\text{N}$, $125\text{--}155^\circ\text{E}$) for the 1991 summer. *Thin solid curve* denotes raw OLR anomalies (indicated by departures from the 1979–1995 base period climatological daily means). *Thick solid curve* is the 20–60-day filtered OLR anomalies. *Thin dashed parallel lines* denote half of one standard deviation of the 20–60-day oscillation. The typhoon symbols indicate the times of initial formation of tropical cyclones within the western North Pacific area

periods. Larger spectral coefficients were observed to concentrate within a broad period range from 20 to 60 days, with statistically significant spectra above 95% confidence level for a red-noise process (Fig. 4), indicating that the 20–60-day oscillation was a dominant mode of convective activity in the western North Pacific. Thus the time series of the 20–60-day filtered OLR anomaly was reconstructed by the inverse transform over all scales between 20 and 60 days (Fig. 3), with 62% of the total variance being explained by this 20–60-day mode. Although the quasi-period range of the 20–60-day oscillation was broader than that of the typical MJO firstly found by Madden and Julian (1971, 1972), such an oscillation was actually a manifestation of the planetary-scale eastward propagating MJO in the western North Pacific (as discussed below). Therefore, in present study, the 20–60-day oscillation was also simply called as the MJO, which was convenient to compare to previous studies such as that of Maloney and Hartmann (2000, 2001). Note also that synoptic-scale disturbances less than 20 days accounted for nearly 32% of the total variance, which might reflect the contributions of tropical cyclones due to their frequent occurrences and movements especially during active MJO phases.

As shown by Mao and Wu (2006), a MJO cycle can be defined as the one with a positive and a negative anomaly (or an active and an inactive phase), both of which must have a peak amplitude greater than half of one standard deviation from zero. According to this criterion, four significant cycles could be identified, with much larger amplitudes during June–August (Fig. 3). Note that two or more tropical cyclones formed successively during each active convection phase of the MJO. For example, there were four and three cyclones generating, respectively, in

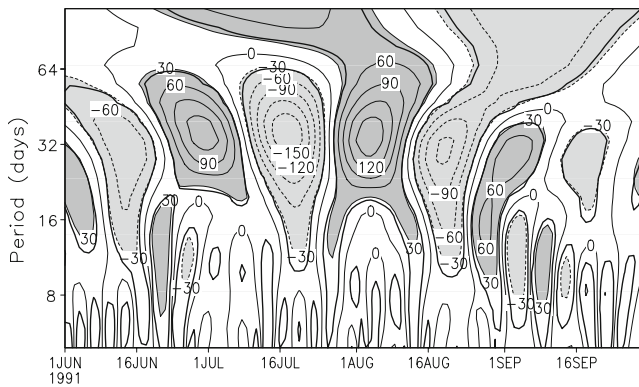


Fig. 4 The wavelet spectrum of the raw OLR anomaly time series shown in Fig. 3. The absolute values of the spectral coefficients greater than 30 are shaded. Thick solid contour encloses regions of greater than 95% confidence for a red-noise process with a lag-1 coefficient of 0.90

mid-July and in mid-August. Tropical cyclones were noted to occur during or before the peaks of active MJO phases. That is, tropical cyclogenesis were most likely to generate during the developing stages of active MJO phases. Note also that the amplitude of the cycle during September was less than those during June–August (Fig. 3), suggesting that there were other timescale disturbances contributing to the variations of tropical cyclogenesis. An oscillation with a period of around 10 days was indeed evident with statistically significant spectra during September (Fig. 4), indicating that the tropical cyclogenesis during this month was modulated by both MJO and the 10-day oscillation. However, tropical cyclogenesis scarcely appeared during inactive MJO phases. As discussed by Kim et al. (2008), such clustering of tropical cyclogenesis within the strong MJO convective envelope in the western North Pacific can support the hypothesis that there are more chances of tropical cyclones being generated by means of Rossby wave dispersion in the wake of a preexisting tropical cyclones (e.g., Sobel and Bretherton 1999).

To demonstrate the association of the 20–60-day oscillation in convection in the western North Pacific with the typical planetary-scale MJO (Madden and Julian 1994; Wheeler and Hendon 2004; Zhang 2005), we have compared the time series of the 20–60-day filtered OLR anomaly shown in Fig. 3 to the all-season real-time multivariate EOF-based MJO index of Wheeler and Hendon (2004, available from <http://www.bom.gov.au/> and www.cpc.noaa.gov). As suggested by Wheeler and Hendon (2004), the first two principal component time series (referred to as RMM1 and RMM2) of the leading EOF modes can be able to represent the essential characteristics of the tropical planetary-scale MJO, and the state of the MJO can be particularly measured in the phase space defined by the RMM1 and RMM2, with eight different

phases of the MJO designated in a global context. Based on the evolution of the EOF-based MJO index in the phase space for 1 June 1991 to 30 September 1991 archived in the former website above, four MJO events were also observed with different intensities indicated by the vector of RMM1 and RMM2. Although the MJO event in July was relatively weak as compared to those in other months, the large amplitudes of greater than 1.0 were still found to exist during the period between phases 5 and 6. Note that this period just corresponded to the time when the enhanced convection occurred in the western Pacific north of the equator. Other three strong MJO events all exhibited large amplitudes between phases 5 and 6. Actually, for each MJO cycle, the time of the large amplitudes occurring in the western North Pacific coincided with the peak phase of the negative 20–60-day convective anomaly shown in Fig. 3, which suggests that the 20–60-day oscillation in convection in the western North Pacific can be ascribed to the arrival of the planetary-scale eastward propagating MJO. The spatial composites of the MJO for different seasons are also archived in the former website above, and these composites are formed by averaging the field data for eight different phases. From the composite of OLR and 850-hPa wind anomalies for the June–September season, it is also found that during phase 6 the active convection accompanied by an anomalous cyclone actually occurs in the western North Pacific, with negative OLR anomalies less than -30 W m^{-2} . Such an anomalous cyclone in the western North Pacific is very similar to that in Fig. 6c (as shown in Section 5). The opposite flow patterns occur during phase 2, with an anomalous anticyclone accompanying the suppressed convection in the western North Pacific as shown in Fig. 6d. These further illustrate that the 20–60-day oscillation in convection and circulation could represent the global tropical MJO activity in the western North Pacific, at least for the 1991 summer. Therefore the MJO was a major agent in modulating repeated development of tropical cyclones in the western North Pacific during the 1991 summer.

4 Tropical cyclogenesis during the active MJO phase

Gray (1968, 1979) described a set of necessary conditions related to tropical cyclone development on seasonal timescales. In addition to warm SST, tropical cyclogenesis occurs favorably in regions of low-level positive vorticity, small vertical wind shear, high mid-tropospheric relative humidity, and non-zero Coriolis force. Thus Liebmann et al. (1994) suggested that the MJO is one of favorable large-scale environmental conditions to produce tropical cyclone clustering. Since tropical cyclogenesis tended to occur during active MJO phases (Fig. 3), the intraseasonal circulations as large-scale, slowly varying anomalies

relative to tropical cyclones should be examined in more details because active and inactive phases of convective activities are directly associated with intraseasonal variations in the low-level circulations in the western North Pacific.

The evolution of the 20–60-day filtered OLR anomalies in Fig. 3 shows that the cycle from 1 July to 4 August exhibited the largest amplitude among the four cycles; thus, this cycle is selected to investigate the tropical cyclogenesis in association with the MJO. Figure 5 illustrates day-by-day evolutions of the 20–60-day structure of both winds and relative vorticity at 850 hPa. For brevity, in Fig. 5, the flow patterns are shown only from 14 to 21 July, with the last three tropical cyclones (indicated by typhoon symbols) generating within this period. As analyzed in Section 3, this period was an active convective phase of the local MJO in the western North Pacific; on the other hand, it coincided with phases 5 and 6 in the phase space of RMM1 and RMM2 (Wheeler and Hendon 2004), corresponding to the global planetary-scale MJO propagating from western maritime continent into the western North Pacific. On 14 July, an anomalous cyclone along with large positive relative vorticity was observed over the Philippine Sea. Associated with this positive vorticity, a large positive vorticity zone was present in a band extending southeastward into the equatorial region from 130° to about 160°E. Actually, such an elongated positive vorticity zone oriented in a southeast–northwest direction was a manifestation of enhanced monsoon trough (as discussed below), representing the active MJO signal. Note that anomalous positive vorticity east of 160°E and north of 10°N resulted from easterly anomalies, with these easterly anomalies being associated with the subtropical western North Pacific high. Subsequently, both westerly anomalies around 10°N on the southern side of the anomalous cyclone and southeasterly anomalies on its eastern side strengthened so that the area with positive vorticity greater than $0.5 \times 10^{-5} \text{ s}^{-1}$ expanded eastward to 140°E by 15 July. A tropical cyclone (eventually Typhoon Amy) thus generated in the southeastern extent of this low-frequency cyclonic circulation at 13.0°N, 138.0°E on 0000 UTC 15 July. This tropical cyclone formed around the southeastern corner of the maximum vorticity where anomalous monsoon westerlies and trade easterlies met directly. Such a confluent zonal flow satisfied the necessary conditions for barotropic instability (as discussed below) and would favor the growth of synoptic-scale disturbances. As shown by Sobel and Bretherton (1999), the region of confluence of the flow in the western Pacific where trade easterlies meet monsoon westerlies produces growth of Rossby waves of approximately 30% per day by a wave accumulation mechanism. During the next 4 days, the low-frequency cyclonic circulation gradually intensified, with large positive vortic-

ity greater than $0.5 \times 10^{-5} \text{ s}^{-1}$ extending further southeastward, indicating an amplification of the MJO. Note that anomalous westerlies and southeasterlies became significantly stronger than those 4 days before. As a result, two tropical cyclones formed one after the other on the southeastern side of the low-frequency cyclone, with the former (eventually Typhoon Brendan) occurring at 11.5°N, 129.0°E on 0000 UTC 20 July and the latter (eventually Typhoon Caitlin) appearing at 12.0°N, 143.5°E on 1200 UTC 21 July. It should be noted that the first cyclone (Typhoon Zeke) in this active period also formed at the eastern edge of the maximum positive vorticity on 1200 UTC 8 July (not shown), but accompanied by easterly anomalies. The above facts suggest that tropical cyclones preferred to form near the eastern end of the maximum positive vorticity of the low-frequency cyclonic circulation during the active MJO phase, consistent with the composite results of Liebmann et al. (1994). They showed that tropical cyclones cluster around the positive low-level vorticity anomaly, with many tropical cyclones occurring in the southeastern octant of the vorticity anomaly as those combined in the other octants (see their Fig. 5a). We have also examined other three active phases and found similar results. These results were in agreement with the findings of Kim et al. (2008), who examined the variability of tropical cyclone activity in the western North Pacific in the various categories of the MJO during summer (June–September) for the period 1979–2004. They found that more tropical cyclones occur when the MJO-related convection center is located in the western North Pacific, with the increase of positive vorticity anomalies being related to an enhanced monsoon confluent zone due to an increase in low-level westerlies. The clustered tropical cyclogenesis was also suggested to be associated with the zonal vertical wind shear. In addition, all of the aforementioned four tropical cyclones formed south of 14.6°N, with two of them in the southeast quadrant, which also accorded with the results of Kim et al. (2008). They showed spatial variations of the major locations of tropical cyclogenesis in the western North Pacific being linked with the propagation of the MJO. When enhanced convection migrates into the western North Pacific, tropical cyclones prefer to occur in both southeast and southwest quadrants, with a statistically significant increase in the number of tropical cyclogenesis in the southeast quadrant during June–July. Note that the tropical cyclone Amy formed on 15 July, which could be attributed to the intensification of monsoon westerlies and trade easterlies and their convergence. But on all the days following 15 July, these conditions were stronger than that on July 15, yet, no tropical cyclone formed until 20 and 21 July (formed in both days). These indicate that tropical cyclones may not always form in the extreme active MJO

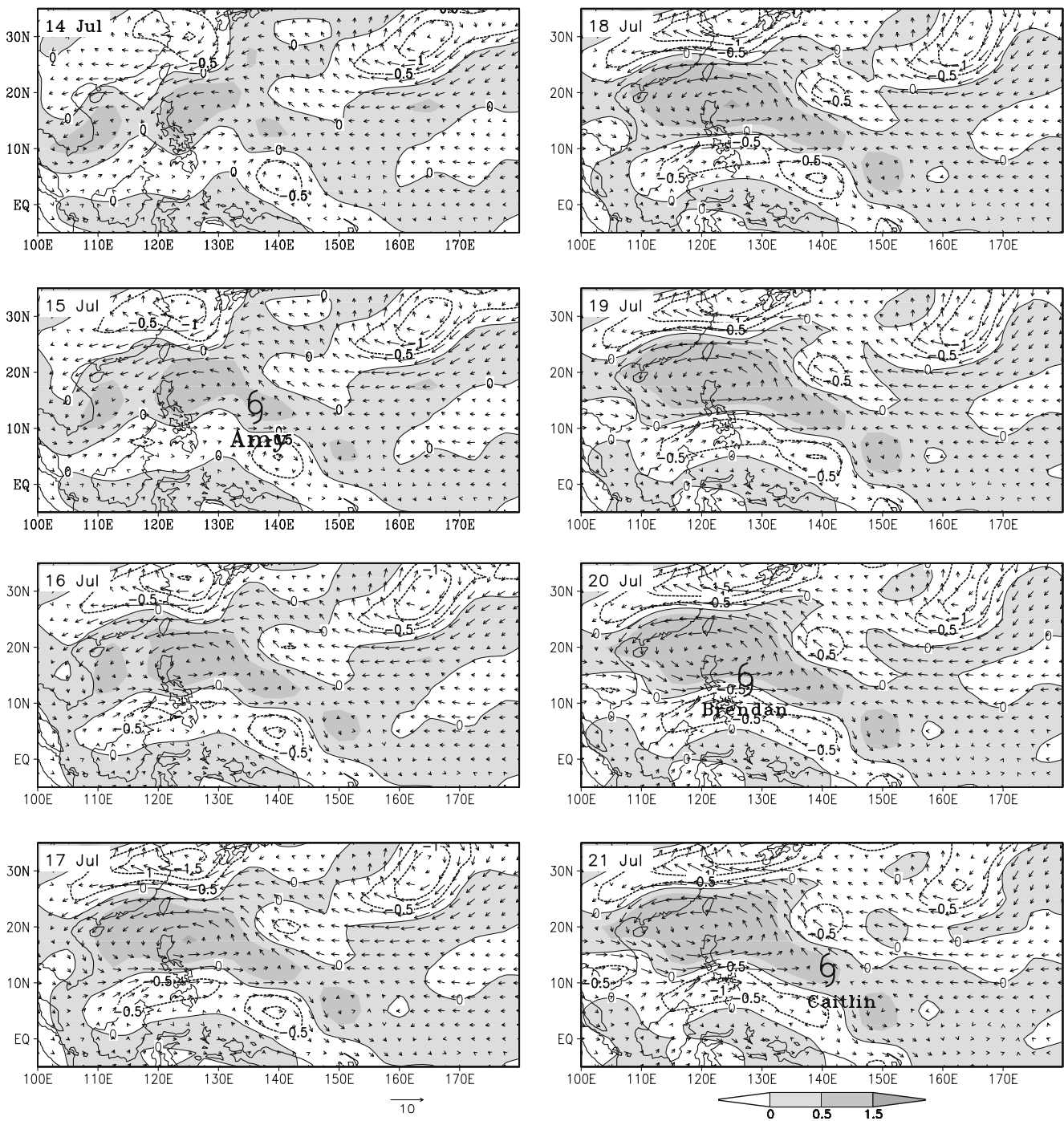


Fig. 5 Evolutions of the 20–60-day filtered 850-hPa wind (vectors, m s^{-1}) and relative vorticity (contours, 10^{-5}s^{-1}) anomalies for an active MJO period from 14 to 21 July 1991. Positive vorticity

anomalies are shaded, with different values indicated in color bar. The initial position of tropical cyclogenesis is denoted by the typhoon symbol, with the tropical cyclone name marked under the symbol

phase, because whether a tropical cyclone forms and when it occurs may depend on other dynamical factors such as interacting mesoscale vortices (Simpson et al. 1997) or vertical wind shear (Maloney and Hartmann 2000) under the background of the favorable large-scale cyclonic

vorticity environment. However, further studies are needed to address these mechanisms. Note also that within this active MJO phase, except for the typhoon Caitlin, other three typhoons made landfall in southern China in the end. This unusual phenomenon also deserves further research.

5 Unstable zonal flow in the monsoon trough

Some previous studies have indicated that most of tropical cyclones develop within or just poleward of the monsoon trough and Inter-Tropical Convergence Zone and have shown evidence for an enhancement of vorticity in the monsoon trough prior to tropical cyclogenesis in the western Pacific (e.g., Gray 1968; Zehr 1992; McBride 1995). Harr and Elsberry (1995) demonstrated that variability in low-level zonal wind anomalies, which signifies strength of the monsoon trough over the western North Pacific, has a significant impact on the location and track characteristics of tropical cyclone activity. Thus, the interaction and fluctuation of easterlies and westerlies that constitute the monsoon trough may represent an important cyclogenesis mechanism in the western Pacific (Briegel and Frank 1997; Sobel and Bretherton 1999).

To reveal the fluctuation of the monsoon trough and understand the enhancement of tropical cyclogenesis during active MJO phases, the composite analyses are made for the four cycles shown in Fig. 3, with the compositing technique as in Mao and Chan (2005). Each MJO cycle is divided into several different phases, and then the average is taken of the variable field occurring for the days that fall within each of phases. Figure 6 presents the unfiltered and filtered 850-hPa

winds for the active and inactive peak phases of the MJO, corresponding to phases 6 and 2 in the phase space of RMM1 and RMM2 (Wheeler and Hendon 2004). The Student *t* test is applied to each wind component to assess the statistical significance of the composite results. During the extreme active phase (Fig. 6a), the unfiltered wind field shows that significantly strong monsoon westerlies prevailing north of the maritime continent converged with strong easterlies, forming an enhanced monsoon trough that stretched from the South China Sea to Philippine Seas west of 150°E. Correspondingly, in the filtered field, a significantly huge cyclonic anomaly dominated much large area spanning from southern China and Indochina Peninsula to 150°E (Fig. 6c), with anomalous westerlies and southeasterlies meeting in the monsoon trough region, leading to a large positive vorticity anomaly (see Fig. 5). The entire flow pattern resembled those in an individual cycle shown in Fig. 5, confirming that the temporal clustering of tropical cyclogenesis was due to enhanced monsoon trough during the active MJO phase. In contrast, during the extreme inactive phase (Fig. 6b), both westerlies and easterlies weakened significantly so that the monsoon trough shrunk westward and became very shallow. In the filtered field, strong northerly and northeasterly anomalies on the eastern side of the huge anticyclonic anomaly

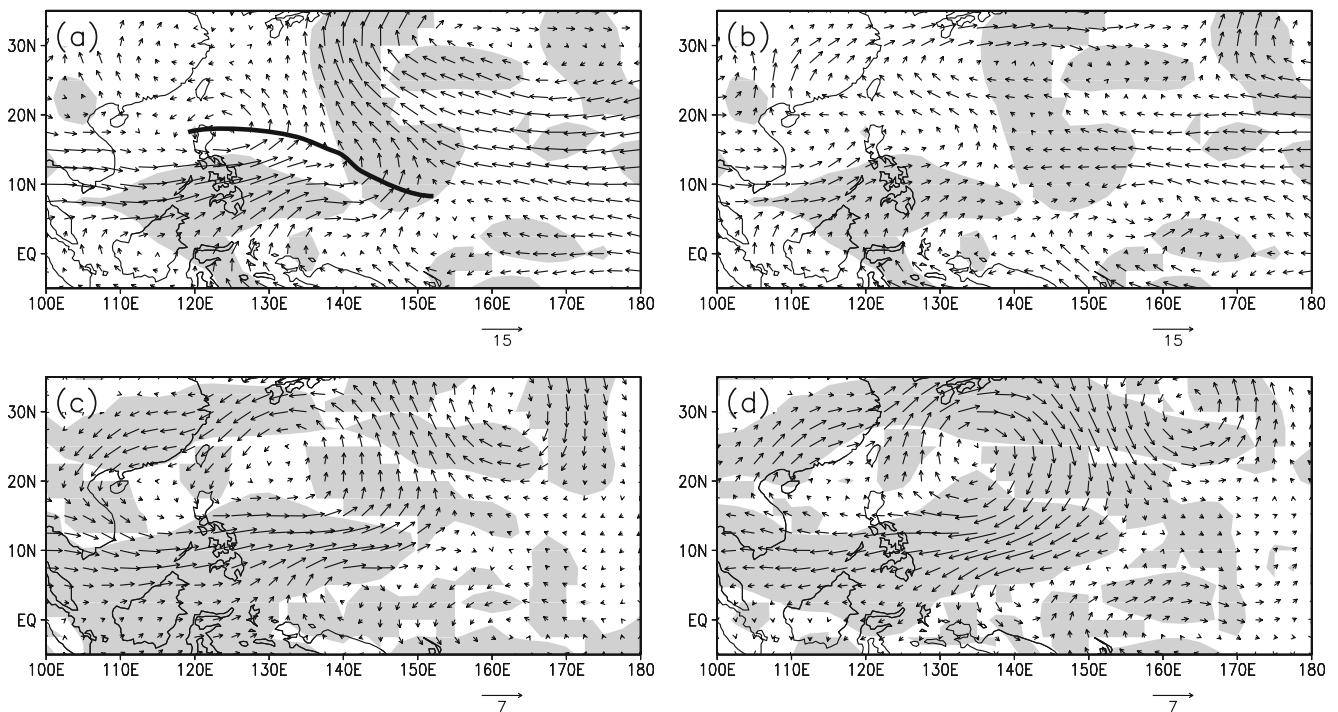


Fig. 6 Composite patterns of unfiltered 850-hPa winds (m s^{-1}) for the **a** active and **b** inactive MJO peak phases. **c** and **d** as in **a** and **b**, except for the 20–60-day filtered 850-hPa winds. *Shadings* denote grid points where the wind differences between the active and inactive MJO peak

phases for **a** and **b** or the wind anomalies during the active and inactive MJO peak phases for **c** and **d** are significantly different from zero at the 95% confidence level (based on the Student's *t* test) in at least one of the wind components (zonal and meridional)

formed a divergent environment in the western North Pacific, which would tend to inhibit tropical cyclone development (Fig. 6d).

Since significant fluctuations appeared in the intensity of the monsoon trough, the basic zonal flow consisting of monsoon westerlies and trade easterlies might be unstable. Molinari et al. (1997) related the dynamically unstable basic state to enhanced tropical cyclogenesis in the eastern Pacific during the active MJO phase. The necessary conditions are therefore examined for barotropic instability of the zonal flow in the monsoon trough region. Figure 7a shows the time-latitude cross section of zonally averaged 850-hPa zonal wind, illustrating the meridional distribution of the zonal flow in the monsoon trough region. Four periods with strong westerly jet greater than 5 ms⁻¹ were found around mid-June, second half of July, mid-August, and first half of September, with strong easterlies to the north. These were four major periods of acceleration of both westerlies and easterlies, with each period well corresponding to the active MJO phase identified by OLR. Note that westerlies during the third period considerably expanded more northward than those during the other periods.

As suggested by Krishnamurti et al. (1981), possible barotropic instability of a zonal flow with horizontal shear can be examined based on the meridional gradient of its absolute vorticity. The zonally averaged meridional gradient of absolute vorticity is given by

$$\langle M \rangle = -\frac{\partial^2}{\partial y^2} \langle u \rangle + \beta \tag{1}$$

where M represents the meridional gradient of absolute vorticity, u is the zonal wind, and β denotes the meridional

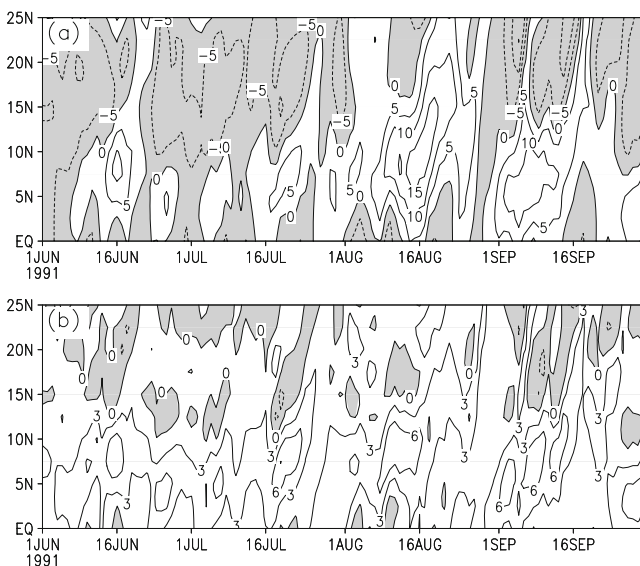


Fig. 7 Time-latitude cross sections of the zonally averaged (125–155°E) 850-hPa **a** zonal flow (m s⁻¹) and **b** meridional gradient (10⁻¹¹ s⁻¹ m⁻¹) of its absolute vorticity. Negative values are shaded

gradient of Coriolis parameter. The angle bracket denotes a zonal average. It is evident that the meridional gradient changed its sign around 10–15°N (Fig. 7b). Note the several significant periods with both positive and negative gradient between 0° and 25°N. These indicate that the zonal flow during these periods was barotropically unstable because it indeed satisfied the necessary condition for barotropic instability with the meridional gradient of absolute vorticity vanishing somewhere on the meridional plane (Kuo 1949). Actually, such an unstable zonal flow also satisfied the additional necessary condition for instability (Fjortoft 1950; Eliassen 1983). This additional condition requires that the mean zonal flow is positively correlated with the meridional gradient of its absolute vorticity. Compared to Fig. 7a, it is found that during each of four persistent periods with both positive gradient to the south and negative gradient to the north, the positive gradient coincided with strong westerlies south of around 10–15°N, while the negative gradient corresponded to strong easterlies to the north, indicating that a positive correlation existed between the mean zonal flow and the meridional gradient. It is obvious that the zonal flow and meridional gradient of absolute vorticity in the monsoon trough region exhibited the same intraseasonal fluctuation as the convective activity. Therefore, the dynamical instability of basic zonal flow may be an important mechanism for tropical cyclogenesis in the western North Pacific, and the intraseasonal oscillation of such an unstable zonal flow may be responsible for the temporal clustering of tropical cyclone formations.

6 Barotropic energy conversion for tropical cyclogenesis

Since the barotropic instability existed in the zonal flow in the western North Pacific during active MJO periods, the contributions of such an unstable basic flow to the growth of synoptic disturbances through barotropic eddy–mean flow interactions will be investigated. Maloney and Hartmann (2001) showed that lower tropospheric barotropic dynamics can provide a significant source of kinetic energy for tropical wave disturbances during MJO westerly periods. Following Maloney and Hartmann (2001), the kinetic energy tendency equation in pressure coordinates for a barotropic fluid, linearized about a basic state (\bar{u}, \bar{v}), can be expressed as

$$\frac{\partial}{\partial t} K' = -\bar{V} \cdot \nabla K' - \bar{u}' \bar{v}' \frac{\partial}{\partial y} \bar{u} - \bar{u}' \bar{v}' \frac{\partial}{\partial x} \bar{v} - \bar{u}'^2 \frac{\partial}{\partial x} \bar{u} - \bar{v}'^2 \frac{\partial}{\partial y} \bar{v} - 2DK' - (\bar{v}' \cdot \nabla \Phi'_a) \tag{2}$$

where \bar{V} is the horizontal wind vector of the basic state flow, (u', v') are the eddy winds, Φ'_a is the part of the

geopotential not in balance with the basic state flow, f is the Coriolis parameter, D is the drag coefficient, and the eddy kinetic energy K' is given by

$$K' = \frac{1}{2} (\overline{u'^2} + \overline{v'^2}) \quad (3)$$

Here, the basic state flow (\bar{u}, \bar{v}) used in the energy computation are the 20-day running-mean winds, which basically represent the intraseasonal flow variation because the seasonal change is small during the calculation period in the same summer. The eddy winds (u', v') are defined as the departures from the basic state flow, and such a definition ensures sufficient scale separation between the basic MJO flow and eddies. Note that synoptic disturbances are totally included within these eddies because the life cycle of a tropical cyclone is evidently less than the eddy timescale.

The first term on the right hand of Eq. 2 denotes the advection of eddy energy by the mean flow, the next four terms are the barotropic conversion terms, $-2DK'$ is the dissipation rate, and the last term is the work done by the eddy geopotential. Of interest here are the barotropic energy conversions; thus, they are separated from the other contributions to the energy tendency,

$$\frac{\partial}{\partial t} K'_{baro} = -\overline{u'v'} \frac{\partial}{\partial y} \bar{u} - \overline{u'v'} \frac{\partial}{\partial x} \bar{v} - \overline{u'^2} \frac{\partial}{\partial x} \bar{u} - \overline{v'^2} \frac{\partial}{\partial y} \bar{v} \quad (4)$$

Figure 8 shows the average 850-hPa eddy kinetic energy for the active and inactive peak phases. The eddy kinetic energy higher than $20 \text{ m}^2 \text{ s}^{-2}$ was observed in the monsoon trough region during the active phase (Fig. 8a), while during the inactive phase the eddy kinetic energy was generally lower than $20 \text{ m}^2 \text{ s}^{-2}$ in the monsoon trough region (Fig. 8b). The distinct energy differences between these two phases occurred in the eastern part of the trough region (Fig. 8c), suggesting more active development of tropical cyclones during convectively active MJO phases than during suppressed phases. This result is supported by the barotropic modeling of Hartmann and Maloney (2001), who showed that tropical eddy kinetic energy is enhanced during westerly wind regimes, particularly in the accumulation zone near the downstream end of the westerly jets.

To highlight the relative importance of the barotropic energy conversion through which synoptic eddies grow from the basic MJO flow, the composite tendency and the composite contribution from each term in Eq. 4 are presented in Fig. 9 for the active peak phases. Strong generation of eddy kinetic energy occurred over the tropical cyclogenesis region ($10\text{--}20^\circ\text{N}$, $125\text{--}155^\circ\text{E}$), with larger generation rate coinciding with the monsoon trough (Fig. 9a). The maximum generation rate was present around eastern end of the monsoon trough ($10\text{--}15^\circ\text{N}$, $145\text{--}155^\circ\text{E}$),

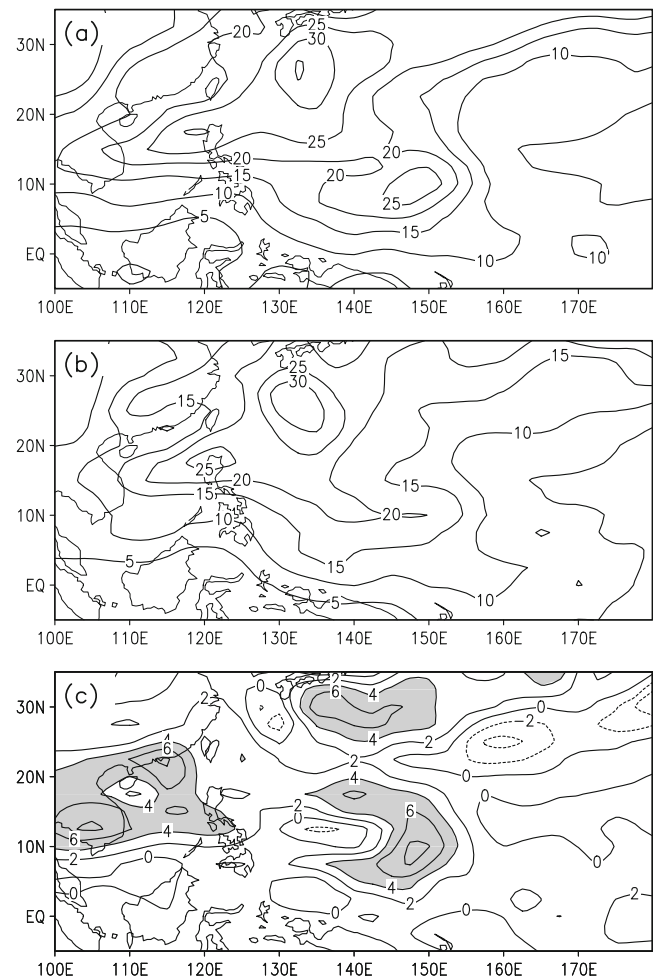


Fig. 8 Composite 850-hPa eddy kinetic energy ($\text{m}^2 \text{ s}^{-2}$) for the **a** active and **b** inactive peak phases and **c** differences between **a** and **b**. Difference values greater than $4 \text{ m}^2 \text{ s}^{-2}$ are shaded

suggesting more synoptic disturbances developing. The secondary generation maxima occurred near the Philippines, which may be attributed to both local tropical cyclogenesis and monsoon intensification. As compared to the active phase, the generation rates of eddy kinetic energy in the monsoon trough region were weak during the inactive phase (not shown). Therefore, barotropic dynamics in the western North Pacific was indeed important to the tropical cyclogenesis.

The eddy kinetic energy generation was dominated by both terms of eddies interacting with zonal and meridional gradients of the basic zonal flow over the western North Pacific ($10\text{--}20^\circ\text{N}$, $125\text{--}155^\circ\text{E}$), especially for the eastern end of the monsoon trough between $145\text{--}155^\circ\text{E}$ (Fig. 9b, d). Conversion process by the zonal convergence term $-\overline{u'^2} \partial \bar{u} / \partial x$ during active MJO phases was substantial in the barotropic energy generation, suggesting the importance of direct confluences of westerlies with easterlies in the

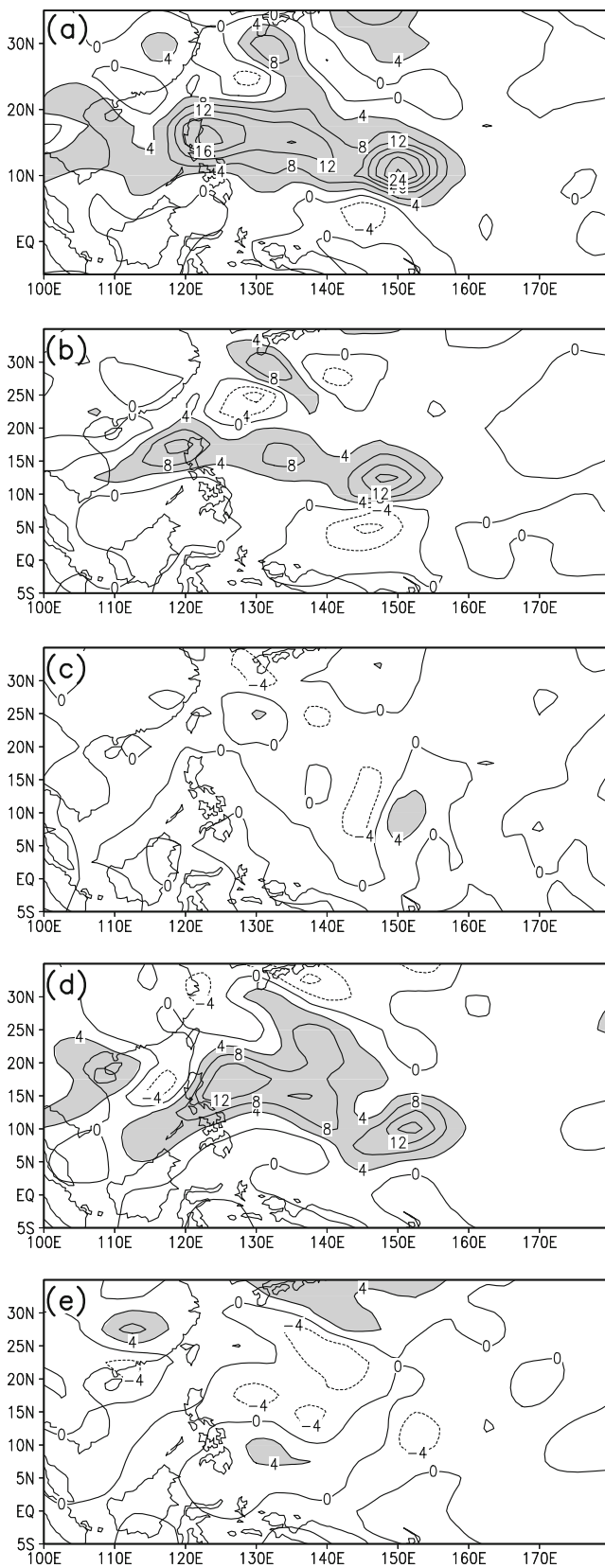


Fig. 9 Composite distributions of **a** time rate of change of eddy kinetic energy at 850 hPa through barotropic conversions from the basic mean flow and associated conversion terms of **b** $-\overline{u'v'}\partial\overline{u'}/\partial y$, **c** $-\overline{u'v'}\partial\overline{v'}/\partial y$, **d** $-\overline{u'^2}\partial\overline{u'}/\partial x$, and **e** $-\overline{v'^2}\partial\overline{v'}/\partial x$ for the active MJO peak phases. Contour interval is $4.0 \times 10^{-5} (\text{m}^2 \text{s}^{-2}) \text{s}^{-1}$. Positive values greater than $4.0 \times 10^{-5} (\text{m}^2 \text{s}^{-2}) \text{s}^{-1}$ are shaded

monsoon trough region, which was in agreement with results of Ritchie and Holland (1999). The magnitude of conversion process by the meridional gradient of zonal flow $-\overline{u'v'}\partial\overline{u'}/\partial y$ was comparable to that of the $-\overline{u'^2}\partial\overline{u'}/\partial x$ term, reflecting the significant contribution of cyclonic shear of the basic zonal flow. Note that there was a maximum center between 130° and 140°E , which was consistent with Maloney and Hartmann (2001). The interactions between eddies and zonal and meridional gradients of the mean meridional wind appeared to have less contributions to the barotropic energy generation (Fig. 9c, e). Therefore, as noted by Lau and Lau (1992), the barotropic conversion could provide a major energy source for the formation and growth of tropical cyclones in the western North Pacific during active MJO phases.

7 Summary and discussion

The objective of this study is to examine the modulation of the western North Pacific tropical cyclogenesis by the MJO during boreal summer. A representative case of such a phenomenon was the activity of tropical cyclones in 1991. During the 1991 summer, tropical cyclogenesis in the western North Pacific exhibited striking fluctuations in the frequency with several distinct active and inactive periods.

The largest subseasonal variance of convective activities was observed in the monsoon trough region where tropical cyclones form most frequently; thus, the dominant intra-seasonal signals were firstly identified based on OLR data. The wavelet analysis shows that significant spectral coefficients were concentrated within a broad period range from 20 to 60 days, with more than half of the total variance explained, indicating that the 20–60-day oscillation was a dominant mode controlling the behaviors of convective activity in the western North Pacific. Such a 20–60-day oscillation in convection was demonstrated to be a manifestation of the planetary-scale eastward propagating MJO in the western North Pacific, with several tropical cyclones forming successively during each active convection phase of the MJO. Tropical cyclones tended to generate near the southeastern corner of the maximum vorticity of the low-frequency cyclonic circulation during the developing and peak stages of the active MJO phase, and this preferential corner was usually the eastern end of enhanced monsoon trough during the active MJO phase. However, tropical cyclogenesis hardly occurred during

inactive MJO phases. Thus, the MJO was a major agent in modulating repeated development of tropical cyclones in the western North Pacific during the 1991 summer.

Since the intraseasonal oscillation in large-scale convection is directly related to that in the low-level circulation over the western North Pacific, the intraseasonal variation of 850-hPa winds is examined in terms of the zonal flow and its instability in the monsoon trough region. The MJO in circulation was characterized by a huge anomalous cyclone (anticyclone) in the lower troposphere existing alternately over the western North Pacific, which regulated a strong (weak) convergence between monsoon westerlies and trade easterlies, leading to an enhanced (weakened) monsoon trough. The zonally averaged 850-hPa zonal wind shows that the MJO in the intensity of the monsoon trough actually reflected the intraseasonal fluctuation of the basic zonal flow, with four major periods of acceleration of both westerlies and easterlies. A westerly jet around 7.5°N was thus characteristic of active MJO phases with strong cyclonic shear of the zonal wind to the north of the jet core. Such a strong large-scale cyclonic shear in the environment of deep convection was favorable for tropical cyclogenesis. An examination of the meridional gradient of absolute vorticity associated with this zonal flow indicates a vanishing of meridional gradient occurring between 10° and 15°N , with a positive correlation existing between the mean zonal flow and the meridional gradient, indicating that the zonal flow in the monsoon trough region satisfied the necessary conditions for barotropic instability. Note that the meridional gradient of absolute vorticity also exhibited the same intraseasonal oscillation as convective activities. Therefore, the dynamically unstable basic flow provided a mechanism for enhanced tropical cyclogenesis in the western North Pacific during active MJO phases.

Energetics analysis indicates that barotropic dynamics was indeed important to the western North Pacific tropical cyclogenesis. The eddy kinetic energy generation was dominated by both terms of eddies interacting with zonal and meridional gradients of the basic zonal flow over the monsoon trough region. Conversion processes by the zonal convergence and by the meridional gradient of the zonal flow during active MJO phases were substantial in the barotropic energy generation, reflecting the important contributions of both direct confluence and cyclonic shear of the basic zonal flow. Thus the barotropic conversion could provide a major energy source for the formation and growth of tropical cyclones in the western North Pacific during active MJO phases.

It should be mentioned that this study has not examined the roles of baroclinic dynamics. As suggested by Maloney and Hartmann (2001), low-level barotropic dynamics cannot explain all aspects of tropical cyclone formation across the Pacific basin. Latent heat release is clearly

important to the developing and mature tropical cyclones, and mature tropical cyclones are characterized by strong vertical shears away from the center. Future work is necessary to investigate the contributions of baroclinic energy conversion to eddy intensification.

As pointed out in the Section 1, the 1991 summer coincided with the developing phase of an El Niño event, with strong MJO events modulating the tropical cyclogenesis in the western North Pacific. Such a significant modulation by the MJO during the 1991 summer was inevitably related to the influence of the El Niño event since ENSO has been found to affect not only the interannual variability of tropical cyclogenesis in the western North Pacific (e.g., Chan 2000; Landsea 2000) but also the characteristics of the MJO (e.g., Hendon et al. 1999; Zhang 2005). Kim et al. (2008) suggested that spatial variations of tropical cyclone activity associated with the MJO during extreme ENSO events depend on the interannual shift of the major genesis location in the western North Pacific, with tropical cyclones during El Niño (La Niña) years largely forming in the southeast (northwest) quadrants. However, how and to what extent the El Niño event affected the location and the MJO behavior of the monsoon trough during the 1991 summer needs to be further studied. Although the 1991 summer could be a representative case with the significant intraseasonal modulation of the tropical cyclogenesis related to ENSO event, whether such a relationship holds true in all other ENSO years deserves further research. Therefore, other similar cases should be examined to better understand the intraseasonal modulation of tropical cyclogenesis by the MJO as well as the effect of ENSO on the modulation. Also investigated in the future should be some associated issues in this case study such as why tropical cyclones do not always generate during the extreme active MJO phases and why tropical cyclones tend to form at the edge of low-frequency cyclonic circulation rather than in the central region.

Acknowledgments NCEP/NCAR reanalysis data used in this study have been obtained from NOAA-CIRES Climate Diagnostics Center, Boulder, Colorado. Tropical cyclone data are obtained from Shanghai Typhoon Institute of China Meteorological Administration. This research is supported by National Basic Research program of China (grants 2006CB403600 and 2005CB42204) and Natural Science Foundation of China grants 40523001 and 40221503.

References

- Bessafi M, Wheeler MC (2006) Modulation of south Indian Ocean tropical cyclones by the Madden-Julian oscillation and convectively coupled equatorial waves. *Mon Weather Rev* 134:638–656
- Briegel LM, Frank WM (1997) Large-scale influences on tropical cyclogenesis in the western North Pacific. *Mon Weather Rev* 125:1397–1413

- Chan JCL (2000) Tropical cyclone activity over the western North Pacific associated with El Niño and La Niña events. *J Clim* 13:2960–2972
- Chan JCL, Ai W, Xu J (2002) Mechanisms responsible for the maintenance of the 1998 South China Sea summer monsoon. *J Meteorol Soc Jpn* 80:367–380
- Chang CP, Chen JM, Harr PA, Carr LE (1996) Northwestward-propagating wave patterns over the tropical western North Pacific during summer. *Mon Weather Rev* 124:2245–2266
- Chen L, Ding Y (1979) An introduction to typhoons in the western Pacific. Science, Beijing
- Chen TC, Weng SP (1998) Interannual variation of the summer synoptic-scale disturbance activity in the western tropical Pacific. *Mon Weather Rev* 126:1725–1733
- Chen TC, Weng SP, Yamazaki N, Kiehne S (1998) Interannual variation in the tropical cyclone formation over the western North Pacific. *Mon Weather Rev* 126:1080–1090
- Dickinson M, Molinari J (2002) Mixed Rossby-gravity waves and western Pacific tropical cyclogenesis. Part I: synoptic evolution. *J Atmos Sci* 59:2183–2196
- Ding Y, Fan H, Xue Q, Chen G (1977) Preliminary study on coinstantaneous developments of multiple typhoons within the intertropical convergence zone. *Chin J Atmos Sci* 2:89–98 (in Chinese)
- Eliassen A (1983) The Charney–Stern theorem on barotropic–baroclinic instability. *Pure Appl Geophys* 121:261–285
- Fjortoft R (1950) Application of integral theorems in deriving criteria of stability for laminar flows and for the baroclinic circular vortex. *Geofis Publ* 17:1–52
- Fu Z, Zhao Q, Qiao F, Liu S (2000) Response of atmospheric low-frequency waves to oceanic forcing in the tropics. *Adv Atmos Sci* 17:569–575
- Gray WM (1968) Global view of the origin of tropical disturbances and storms. *Mon Weather Rev* 96:669–700
- Gray WM (1979) Hurricanes: Their formation, structure, and likely role in the tropical circulation. In: Shaw DB (eds) *Meteorology over the Tropical Oceans*. Royal Meteorology Society, pp 155–218
- Hall JD, Matthews AJ, Karoly DJ (2001) The modulation of tropical cyclone activity in the Australian region by the Madden–Julian oscillation. *Mon Weather Rev* 129:2970–2982
- Harr PA (2006) Temporal clustering of tropical cyclone occurrence on intraseasonal time scales. 27th Conference on Hurricanes and Tropical Meteorology, American Meteorological Society, Monterey, CA
- Harr PA, Elsberry RL (1995) Large-scale circulation variability over the tropical western North Pacific part I: spatial patterns and tropical cyclone characteristics. *Mon Weather Rev* 123:1225–1246
- Hartmann DL, Maloney ED (2001) The Madden–Julian oscillation, barotropic dynamics, and North Pacific tropical cyclone formation part II: stochastic barotropic modeling. *J Atmos Sci* 58:2559–2572
- Hendon HH, Liebmann B (1994) Organization of convection within Madden–Julian oscillation. *J Geophys Res* 99:8073–8083
- Hendon HH, Zhang C, Glick JD (1999) Interannual variation of the Madden–Julian oscillation during austral summer. *J Clim* 12:2538–2550
- Holland GJ (1995) Scale interaction in the western Pacific monsoon. *Meteorol Atmos Phys* 56:57–79
- Kalnay E, Coauthors (1996) The NCEP/NCAR 40-year reanalysis project. *Bull Am Met Soc* 77:437–471
- Kim JH, Ho CH, Kim HS, Cui CH, Park SK (2008) Systematic variation of summertime tropical cyclone activity in the western North Pacific in relation to the Madden–Julian oscillation. *J Clim* 15:1171–1191
- Krishnamurti TN, Ardanuy P, Ramanathan Y, Pasch R (1981) On the onset vortex of the summer monsoons. *Mon Weather Rev* 109:344–363
- Kuo HL (1949) Dynamical instability of two-dimensional non-divergent flow in a barotropic atmosphere. *J Meteorol* 6:105–122
- Landsea CW (2000) El Niño/Southern oscillation and the seasonal predictability of tropical cyclones. In: Diaz HF, Markgraf V (eds) *El Niño and the southern oscillation: multiscale variability and global and regional impacts*. Cambridge University Press, New York, pp 149–181
- Lau KH, Lau NC (1992) The energetics and propagation dynamics of tropical summertime synoptic-scale disturbances. *Mon Weather Rev* 120:2523–2539
- Liebmann B, Smith CA (1996) Description of a complete (interpolated) outgoing longwave radiation dataset. *Bull Am Meteorol Soc* 77:1275–1277
- Liebmann B, Hendon HH, Glick JD (1994) The relationship between tropical cyclones of the western Pacific and Indian Oceans and the Madden–Julian oscillation. *J Meteorol Soc Jpn* 72:401–411
- Madden RA, Julian PR (1971) Detection of a 40–50 day oscillation in the zonal wind in the tropical Pacific. *J Atmos Sci* 28:702–708
- Madden RA, Julian PR (1972) Description of global-scale circulation cells in the tropics with a 40–50 day period. *J Atmos Sci* 29:1109–1123
- Madden RA, Julian PR (1994) Observations of the 40–50 day tropical oscillation—a review. *Mon Weather Rev* 122:814–837
- Maloney ED, Hartmann DL (2000) Modulation of eastern North Pacific hurricanes by the Madden–Julian oscillation. *J Clim* 13:1451–1460
- Maloney ED, Hartmann DL (2001) The Madden–Julian oscillation, barotropic dynamics, and North Pacific tropical cyclone formation, part I: observations. *J Atmos Sci* 58:2545–2558
- Mao J, Chan JCL (2005) Intraseasonal variability of the South China Sea summer monsoon. *J Clim* 18:2388–2402
- Mao J, Wu G (2006) Intraseasonal variations of the Yangtze rainfall and its related atmospheric circulation features during the 1991 summer. *Clim Dyn* 27:815–830
- McBride JL (1995) Global perspectives on tropical cyclones, Report No TCP-38. World Meteorological Organization, Geneva
- McBride JL, Zehr R (1981) Observational analysis of tropical cyclone formation. Part II: comparison of non-developing versus developing systems. *J Atmos Sci* 38:1132–1151
- McPhaden MJ (1993) TOGA-TAO and the 1991–93 El Niño–Southern oscillation event. *Oceanography* 6:36–44
- Molinari J, Knight D, Dickinson M, Vollaro D, Skubis S (1997) Potential vorticity, easterly waves, and tropical cyclogenesis. *Mon Weather Rev* 125:2699–2708
- Molinari J, Vollaro D, Skubi S, Dickinson M (2000) Origins and mechanisms of eastern Pacific tropical cyclogenesis: a case study. *Mon Weather Rev* 128:125–139
- Nakazawa T (1986) Intraseasonal variations of OLR in the tropics during the FGGE year. *J Meteorol Soc Jpn* 64:17–33
- Norquist DC, Recker EE, Reed RJ (1977) The energetics of African wave disturbances as observed during phase III of GATE. *Mon Weather Rev* 105:334–342
- Ren F, Wu G, Dong W, Wang X, Wang Y, Ai W, Li W (2006) Changes in tropical cyclone precipitation over China. *Geophys Res Lett* 33:L20702. doi:10.1029/2006GL027951
- Ritchie EA, Holland GJ (1999) Large-scale patterns associated with tropical cyclogenesis in the western Pacific. *Mon Weather Rev* 127:2027–2043
- Simpson J, Ritchie E, Holland GJ, Halverson J, Stewart S (1997) Mesoscale interactions in tropical cyclone genesis. *Mon Weather Rev* 125:2643–2661
- Sobel AH, Bretherton CS (1999) Development of synoptic-scale disturbances over the summertime tropical northwest Pacific. *J Atmos Sci* 56:3106–3127

- Takayabu YN, Nitta T (1993) 3–5 day period disturbances coupled with convection over the tropical Pacific Ocean. *J Meteorol Soc Jpn* 71:221–245
- Thorncroft CD, Hoskins BJ (1994a) An idealized study of African easterly waves. I: a linear view. *Q J R Meteorol Soc* 120:953–982
- Thorncroft CD, Hoskins BJ (1994b) An idealized study of African easterly waves. II: a nonlinear view. *Q J R Meteorol Soc* 120:983–1015
- Torrence C, Compo GP (1998) A practical guide to wavelet analysis. *Bull Am Met Soc* 79:61–78
- Wheeler M, Kiladis GN (1999) Convectively coupled equatorial waves: analysis of clouds and temperature in the wavenumber–frequency domain. *J Atmos Sci* 56:374–399
- Wheeler MC, Hendon HH (2004) An all-season real-time multivariate MJO index: development of an index for monitoring and prediction. *Mon Weather Rev* 132:1917–1932
- Zehr RM (1992) Tropical cyclogenesis in the western North Pacific. NOAA Tech. Rep. NESDIS 61, Department of Commerce, Washington DC
- Zhang C (2005) Madden–Julian oscillation. *Rev Geophys* 43: RG2003. doi:[10.1029/2004RG000158](https://doi.org/10.1029/2004RG000158)